Evidence for a conducting surface ground state in high-quality single crystalline FeSi

Yuankan Fang[a,b], Sheng Ran[c,1], Weiwei Xie[d], Shen Wang[e], Ying Shirley Meng[e], and M. Brian Maple[a,b,c,2]

[a]Materials Science and Engineering Program, University of California, San Diego, La Jolla, CA 92093; [b]Center for Advanced Nanoscience, University of California, San Diego, La Jolla, CA 92093; [c]Department of Physics, University of California, San Diego, La Jolla, CA 92093; [d]Department of Chemistry, Louisiana State University, Baton Rouge, LA 70803; and [e]Department of NanoEngineering, University of California, San Diego, La Jolla, CA 92093

Contributed by M. Brian Maple, July 3, 2018 (sent for review April 23, 2018; reviewed by Filip Ronning and Brian C. Sales)

We report anomalous physical properties of high-quality single-crystalline FeSi over a wide temperature range of 1.8–400 K. The electrical resistivity $\rho(T)$ can be described by activated behavior with an energy gap Δ = 57 meV between 150 and 67 K, below which the estimated energy gap is significantly smaller. The magneto-resistivity and Hall coefficient change sign in the vicinity of 67 K, suggesting a change of dominant charge carriers. At ∼19 K, $\rho(T)$ undergoes a cross-over from semiconducting to metallic behavior which is very robust against external magnetic fields. The low-temperature metallic conductivity depends strongly on the width/thickness of the sample. In addition, no indication of a bulk-phase transition or onset of magnetic order is found down to 2 K from specific heat and magnetic susceptibility measurements. The measurements are consistent with one another and point to complex electronic transport behavior that apparently involves a conducting surface state in FeSi at low temperatures, suggesting the possibility that FeSi is a 3D topological insulator.

FeSi | surface conductivity | topological insulator | metal-semiconductor transition

The transition metal silicides FeSi, MnSi, CoSi, and CrSi have the B20 crystal structure, which is the only group in the cubic system without an inversion center. These compounds exhibit a rich variety of physical phenomena that are of great interest for fundamental understanding and potential applications. For example, the d-electron compound FeSi shows a remarkable similarity to f-electron Kondo insulators, and the electrical resistivity $\rho(T)$ evolves continuously with decreasing temperature from metallic behavior ($d\rho/dT > 0$) to semiconducting behavior ($d\rho/dT < 0$) (1–5). A considerable amount of theoretical effort (6–10) has been expended to explain the strong temperature dependence of the magnetic susceptibility $\chi(T)$ of FeSi, which reaches a maximum value at ∼500 K (1) that is not due to magnetic order (11, 12).

The ground state of FeSi is considered to be nonmagnetic; however, experimental investigations of FeSi at low temperature reveal features that are sample-dependent and not well understood (5, 13, 14). The published results are consistent in terms of the small semiconducting energy gap of 50–60 meV inferred from $\rho(T)$ measurements in the temperature range 70–170 K. However, upon further decrease of the temperature, the following features in $\rho(T)$ of FeSi have been reported: saturation steps (5); a hump (shoulder) at 70 K (14, 15) or ∼ 35 K (16); a moderate increase with decreasing temperature <40 K (17) or 50 K (18); or a saturation below ∼5 K (19). Moreover, the values of $\rho <$ 70 K reported in these references are also very different, indicating strong sample dependence of the electrical transport behavior. It has been well established in experiments that the electrical properties of semiconductors can be very sensitive to external dopants (20–24). To investigate the intrinsic physical properties of FeSi, we prepared high-quality single-crystal samples of FeSi and performed various types of measurements over a wide temperature range of 1.8–400 K. Anomalous electrical transport behavior associated with a change in primary charge carriers and negative magneto-resistivity at low temperatures was observed in all of the samples. We also report metallic conducting behavior of FeSi single crystals below ∼20 K, yielding evidence for a conducting surface state, consistent with specific heat, magneto-resistivity, and magnetization measurements.

Results and Discussion

The FeSi single crystals grow along the [111] direction in the Sn flux, resulting in bar-shaped samples. The results of single-crystalline X-ray diffraction measurements on FeSi are shown in Fig. 1. Consistent with previous studies, stoichiometric FeSi crystallizes in the cubic chiral structure with space group $P2_13$ ($B20$-type) and lattice parameter a = 4.4860(5) Å. No vacancies were observed according to the refinement. The profile residual Rp was 1.79% with a weighted profile residual Rwp = 4.11%. No electron density residual was detected, revealing the high quality of the FeSi crystals. Scanning electron microscope (SEM) and energy dispersive X-ray spectroscopy (EDX) investigations yielded no evidence of additional elements (*SI Appendix*, Figs. S1–S4).

Because of their bar shape and high quality, the FeSi single crystals are very suitable for electron transport measurements along the [111] direction. Upon cooling from 400 K, metallic-like behavior could be observed down to 336 K, below which the

Significance

The compound FeSi has been the focus of intense research efforts due to its unusual electrical, magnetic, and lattice properties, which are not well understood. This study reveals a semiconducting-to-metallic cross-over with decreasing temperature at ∼19 K, which is not accompanied by any bulk features, in single-crystal samples of FeSi. The low-temperature metallic behavior can be significantly enhanced by reducing the width/thickness of the sample. Application of an external magnetic field easily suppresses the electrical resistivity at low temperatures, but does not have a noticeable effect on the temperature below which metallic conduction occurs. Evidence for a conducting surface state on FeSi similar to the surface state on a topological insulator is presented.

Author contributions: Y.F. and M.B.M. designed research; Y.F., S.R., W.X., S.W., and Y.S.M. performed research; Y.F. and M.B.M. analyzed data; and Y.F., W.X., and M.B.M. wrote the paper.

Reviewers: F.R., Los Alamos National Laboratory; and B.C.S., Oak Ridge National Laboratory.

The authors declare no conflict of interest.

[1]Present address: Department of Materials Science and Engineering, University of Maryland, College Park, MD 20742.

[2]To whom correspondence should be addressed. Email: mbmaple@ucsd.edu.

This article contains supporting information online at www.pnas.org/lookup/suppl/doi:10.1073/pnas.1806910115/-/DCSupplemental.

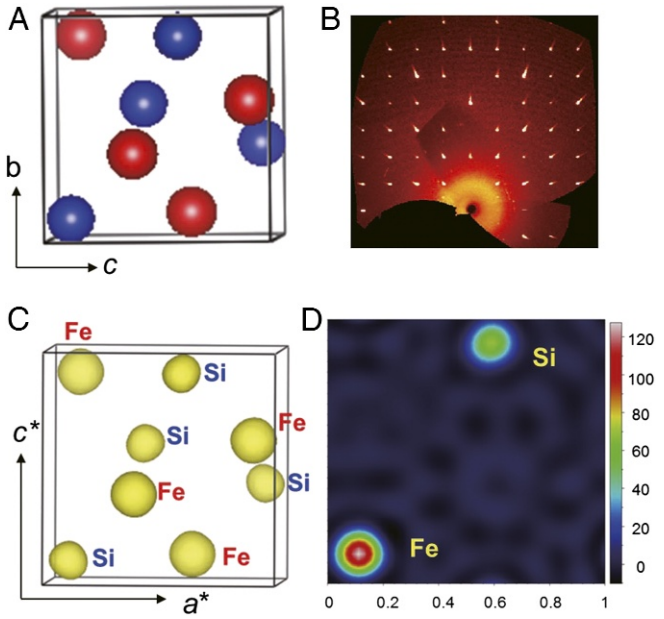

Fig. 1. (*A*) The crystal structure of FeSi (red, Fe; blue, Si). (*B*) Single-crystal X-ray diffraction precession image of the (*h0l*) plane in the reciprocal lattice of FeSi at 300 K. All of the resolved spots correspond to the cubic chiral crystal structure $P2_13$. (*C*) A 3D Fourier map showing the electron density in *B*20-FeSi. (*D*) A 2D Fourier map showing the electron density on Fe and Si along the *z* axis.

resistivity increased with decreasing temperature, resulting in a minimum in $\rho(T)$ at T_{min} = 336 K (Fig. 2*A*, *Inset*). Similar features can also be found in other references with values of T_{min} mostly in the range of 150–300 K) (5, 25–27). Decreasing the temperature further resulted in a gradual enhancement of semiconducting behavior down to 152 K, which has been reported to be related to the opening of an energy gap (28–30).

Fig. 2*B* shows a linear relation of $\ln(\rho)$ vs. $(1/T)$ for FeSi in the temperature range 152 K (T_1) to 67 K (T_2), consistent with standard activated behavior with an energy gap Δ = 57.1 meV; this value of Δ is comparable to reported gap values of 50–60 meV (1, 3, 15, 18). From 54 to 30 K, where the relation $\ln(\rho)$ vs. $1/T$ is also linear, the value of $d\ln(\rho)/d(1/T)$ corresponds to an energy gap of 35 meV. Below 30 K (T_3), the $\rho(T)$ curve cannot be described by a standard activation model. Further decrease of the temperature <19 K resulted in a cross-over from semiconducting to metallic behavior (T_4), as shown in Fig. 2*A*. As the behavior observed in $\rho(T)$ below T_4 was quite different from that reported for FeSi in other references, we repeated the measurements on different FeSi single crystals, which yielded consistent resistivity values at high temperatures. However, a strong size dependence of the metallic conductivity could be observed at low temperatures, as shown in Fig. 3; as the average width/thickness (W) of the sample was reduced, the low temperature metallic conductivity increased dramatically, and the semiconducting-to-metallic cross-over temperature (indicated by the dashed arrow in Fig. 3) gradually increased. In contrast, the electrical resistivity of the FeSi did not have a noticeable dependence on L, the effective length of the sample (the distance between the two voltage leads). As the surface area to volume ratio increased with the thinning of the samples, the results strongly suggest that the metallic conductivity originates from the FeSi surface.

In an effort to gain a better understanding of the temperature dependence of $\rho(T)$ of FeSi, especially the low-temperature metallic behavior, we performed specific heat $C_p(T)$ measurements on the samples down to 1.8 K, the results of which are shown in Fig. 4. It should be mentioned that some of the early reports showed additional features in $C_p(T)$ at ~10 K or <1 K which were attributed to Schottky-like anomalies (5, 19). However, in this study, no Schottky-like features were found in $C_p(T)$. Thus, it is reasonable to describe the specific heat of the samples as the sum of electronic and lattice contributions at low temperatures (i.e., $C_p = \gamma T + \beta T^3$). No anomalies around T_2 = 67 K, T_3 = 30 K, and T_4 = 19 K could be observed, indicating the absence of any bulk phase transitions in FeSi at these temperatures. The estimated value of the Debye temperature θ_D of 457 K lies within the reported range of 377–515 K (5, 31, 32). On the other hand, the electronic specific heat coefficient γ was estimated to be 0.41 $mJ \cdot mol^{-1} \cdot K^{-2}$, which is only ~8–30% of reported values (5), suggesting that the samples studied in this work had a lower concentration of electron donor impurities, as the value of γ was proportional to the density of electronic states at the Fermi level. The metallic-like conduction below T_4 exhibited by the FeSi samples in this work was dramatically different from the semiconducting behavior observed in other FeSi samples which have higher concentrations of charge carriers. The seemingly contradictory phenomena suggest that the metallic conduction observed in this study is unlikely to be a bulk phenomenon, which is also supported by the absence of features indicative of phase transitions in the $C_p(T)$ data.

The temperature dependence of the magnetic susceptibility $\chi(T)$ for FeSi is shown in Fig. 5. Above 100 K, the value of the

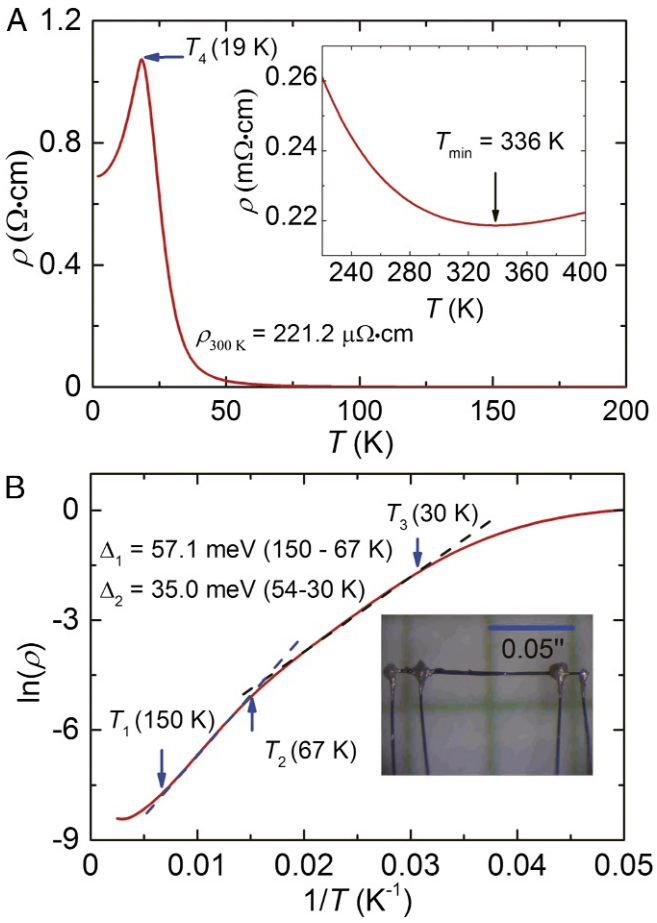

Fig. 2. (*A*) Electrical resistivity ρ vs. temperature *T* for FeSi with the current flowing along the [111] direction <200 K. (*B*) $\ln(\rho)$ vs. 1/*T*. *A* and *B*, *Insets* show the resistivity at high temperatures and a picture of the sample with the four-wire electrical lead configuration, respectively.

magnetic susceptibility increased with increasing temperature, which is similar to the behavior of $\chi(T)$ for an antiferromagnet at temperatures below the Néel temperature. In the temperature range 20–100 K, $\chi(T)$ was very small ($\sim$0.15 emu·mol$^{-1}\cdot$T^{-1}), indicating that FeSi had a very weak response to the external magnetic field and a nonmagnetic ground state. Below 15 K, $\chi(T)$ of FeSi had a Curie–Weiss-like upturn with decreasing temperature, which is apparently associated with magnetic impurities (1, 11). In this study, however, the magnitude and the onset temperature of the $\chi(T)$ upturn was significantly smaller and lower, respectively, than reported values (15, 16, 33), indicating lower magnetic impurity concentration for the present samples. The knee observed in the $M(H)$ curve at $\sim$2 T indicated by the arrow in Fig. 5, *Inset* is also consistent with a paramagnetic impurity scenario. Above 2 T, it seemed that the magnetic field did not dramatically affect the magnetization of the samples, which also suggests the absence of magnetic order at low temperatures. The results of the magnetic measurements revealed that the samples were of high quality, and the features observed around T_2 and T_4 in the $\rho(T)$ curve were not related to any bulk magnetic transitions.

In this study, the magnetization of FeSi can be well described by the following Langevin function:

$$M = M_S[coth(\mu H/k_B T) - k_B T/\mu H], \qquad [1]$$

in which μ is the magnetic moment of the impurity clusters and M_S is the saturation magnetization. The corresponding fitting of $M(H)$ at 3.5 K gives $M_s = 2.433\times10^{20}$ μ_B/mol and μ = 7.95 μ_B. If we assume that the magnetic moment per impurity atom is $3\mu_B$ as in pure iron, the concentration of Fe impurity atoms is only $\sim$130 ppm per Fe atom, which is comparable to or significantly lower than the impurity concentration estimated for single crystal specimens of FeSi (11, 19, 33). The fitting results also show that, on average, only $\sim$2–3 magnetic impurity atoms comprise each cluster, indicating atomic-size magnetic clusters. The estimated value of the Wilson–Sommerfeld ratio of FeSi is $\sim$2.5, using the base magnetic susceptibility $<$100 K and the electronic specific heat coefficient obtained in this study, which is slightly higher than the expected value of $\sim$2 for the Kondo model (34).

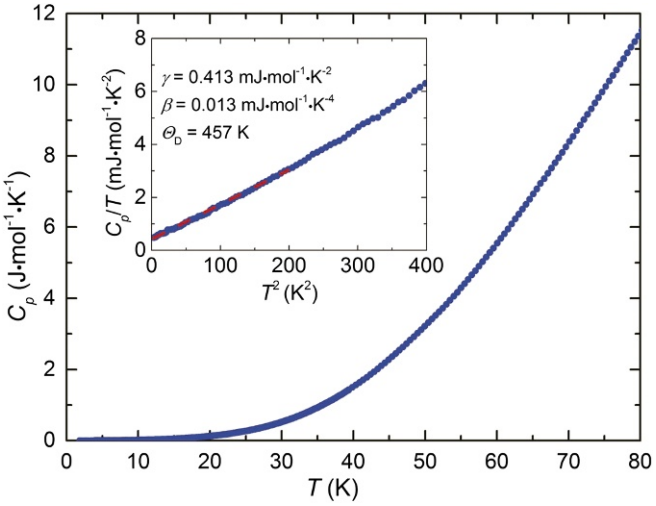

Fig. 4. Specific heat $C_p(T)$ of FeSi at low temperatures from 1.8 to 80 K. A plot of C_p/T vs. T^2 $<$20 K is shown in *Inset*. The dashed line in *Inset* is a fit of the expression $C_p/T = \gamma + \beta T^2$ to the data with the values of γ, β, and θ_D given in *Inset*.

Fig. 6 shows $\rho(T)$ data for FeSi under external magnetic field. At high temperatures, the values of ρ are almost independent of the applied magnetic field; however, a negative magneto-resistivity (MR), where $MR = (\rho_{3T} - \rho_{0T})/\rho_{0T}$, could be observed at $\sim$70 K, as indicated by the arrow in Fig. 5, *Inset* that becomes very significant $<$30 K; these temperatures are very close to the temperatures T_2 = 67 K and T_3 = 30 K, respectively. It should be mentioned that previous studies of the MR are not consistent: A negative MR was reported by Paschen et al. $<$30 K and attributed to quantum interference effects (5); however, a change of sign at $\sim$70 K (close to T_2 = 67 K in this study) was reported later, below which the MR is positive (14). In this study, the negative MR reaches a minimum value at T_4. The peak in the absolute value of the MR in this study is $\sim$20%, which is obviously higher than the peak in the absolute value of the MR reported in refs. 5 and 14, revealing the sample dependence of the MR. While $\rho(T)$ is very sensitive to the applied field at low temperatures, the value of T_4 seems to be independent of H,

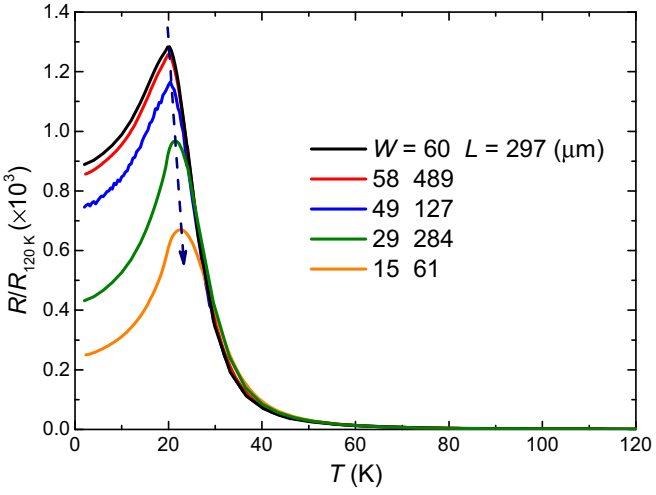

Fig. 3. Temperature dependence of the resistance (R) for FeSi single crystals with different size, normalized by the resistance at 120 K (R_{120}). The symbols W and L refer to the average width/thickness and effective length of the samples, respectively. The arrow indicates the increase of the semiconducting-to-metallic cross-over temperature.

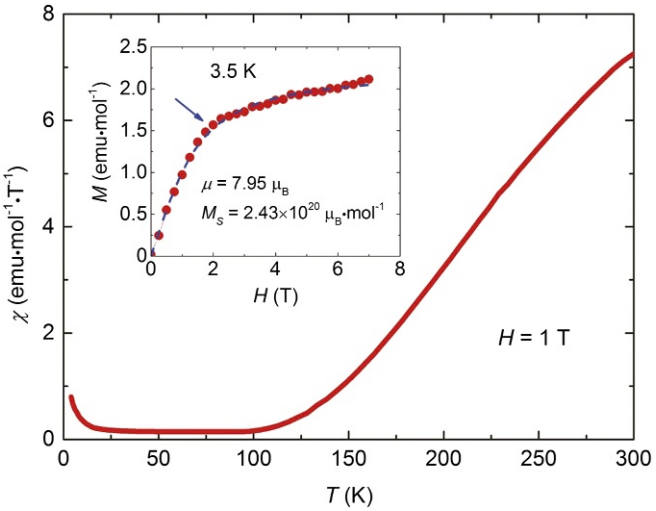

Fig. 5. Magnetic susceptibility χ vs. temperature T for FeSi single crystals. The corresponding magnetization curve at 3.5 K is shown in *Inset*. The dashed curve is a fit of the Langevin function to the $M(H)$ data.

which provides additional evidence that the emergence of metallic conductivity in $\rho(T)$ around T_4 is very robust with respect to the external magnetic field.

The evolution of ρ as a function of H with H perpendicular and parallel to the long axis of the FeSi crystal at 2 K is shown in Fig. 6, *Upper Inset*. No noticeable hysteresis in the H dependence of the resistivity was observed, indicating no detectable free Fe impurities. The value of ρ was suppressed with increasing field, but the evolution of $\rho(H)$ deviated slightly from a linear relation. The angle between the directions of the applied field and the current (long axis of the sample) α had a small effect on the behavior of $\rho(H)$. This can be qualitatively understood by considering both bulk and surface electron conduction for FeSi. The negative MR can be observed at temperature T_2 which is far above T_4, suggesting that the negative MR is a bulk phenomenon. If we assume that the response of the surface contribution to the resistivity to an external field was positive due to the additional scattering of free electrons by the Lorentz force, increasing α will increase the effective applied field on the sample surface and thus slightly enhance the MR.

The main results of the Hall effect measurements at temperatures down to 30 K are displayed in Fig. 7. Unlike the results of previous reports (5), linear relations of the Hall resistivity vs. applied external field can be seen up to 9 T over a wide temperature range >30 K (Fig. 7, *Inset*). At high temperatures, the Hall coefficient R_H was positive and increased slightly with decreasing temperature, indicating that the dominant charge carriers were holes. However, a change of sign in R_H was observed at ~68 K, which is very close to $T_2 = 67$ K and to the temperature of the sign change of the MR. The phenomena observed in the $R_H(T)$, $MR(T)$, and $\rho(T)$ measurements were consistent with one another, indicating that the resistivity is dominated by electron conduction and is sensitive to external field below $T_2 = 67$ K.

Summary

In summary, the following conclusions can be drawn from this study:

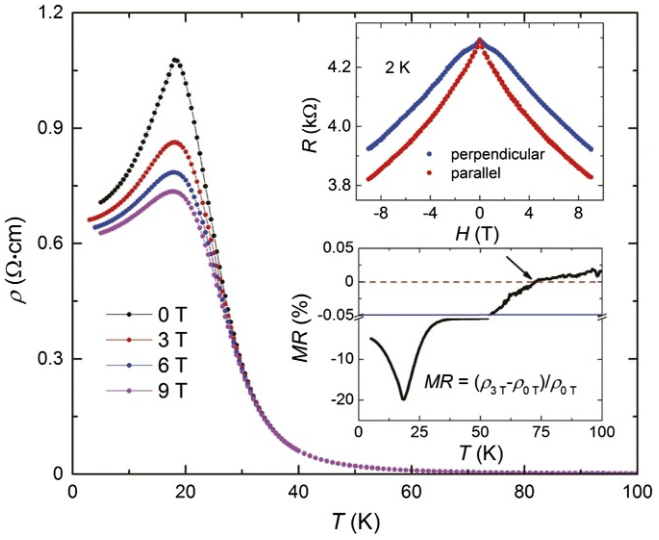

Fig. 6. Electrical resistivity ρ vs. temperature T in magnetic fields up to 9 T. The applied field is perpendicular to the current. Shown in *Upper Inset* is ρ vs. H at 2 K, with the applied fields perpendicular (blue) and parallel (red) to the current, respectively. Displayed in *Lower Inset* is the temperature dependence of the magneto-resistance (*MR*). The definition of the *MR* is given in *Lower Inset*.

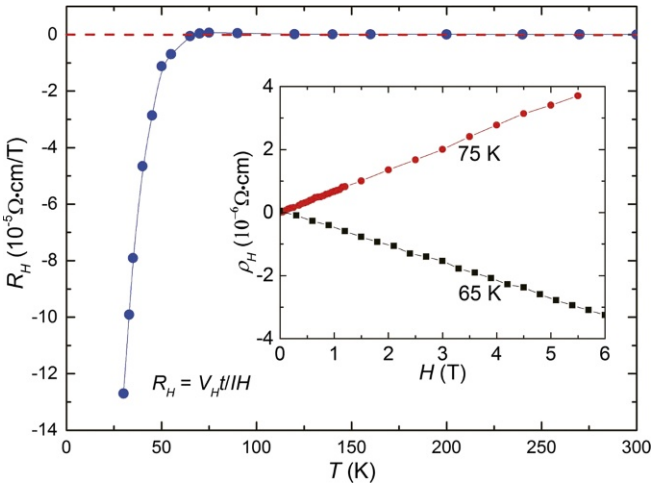

Fig. 7. Evolution of the Hall coefficient R_H with temperature T. The Hall resistivity ρ_H vs. H at 65 and 75 K is shown in *Inset*.

i) The electron transport behavior of FeSi is very sensitive to sample quality. The high quality of the single crystal samples used in this study is supported by X-ray diffraction, dispersive X-ray spectroscopy, specific heat, and magnetization measurements.

ii) In the temperature range 150 to 67 K, the semiconducting energy gap is 57 meV. Below 67 K, a much smaller energy gap and a sign change of the magneto-resistance and Hall coefficient are observed, suggesting a change in dominant charge carriers.

iii) A further decrease of the temperature results in a sharp reversible cross-over from a negative slope to a positive slope of $\rho(T)$ at ~19 K. Corresponding magnetization and magneto-resistivity measurements suggest that there is no bulk magnetic order associated with this slope change in $\rho(T)$. No feature can be observed in specific heat measurements. Investigation of the dependence of the electrical resistivity on the geometrical factor reveals that the metallic conductivity increases dramatically in thinner samples. These results suggest that the metallic conductivity below T_4 is a surface phenomenon. The possibility that FeSi is a 3D topological insulator should be considered for further research.

iv) The fact that T_4 shows no noticeable change with applied external field up to 9 T and that the resistivity below T_4 is not strongly dependent on α imply that the metallic conducting state of FeSi is very robust with respect to external magnetic field.

v) Since the surface conduction of FeSi is very robust under magnetic field and is significant only <19 K, the negative magneto-resistivity of the sample should be associated with the bulk properties of the samples. The slight increase of MR with increasing α should be attributed to the surface state of FeSi.

Methods

Single-crystalline samples of FeSi were grown in a high-temperature Sn flux with Fe:Si molar ratio of 1:1. The quality of the FeSi samples was assessed by means of single-crystal X-ray diffraction at room temperature. A Bruker Apex II X-ray diffractometer with Mo $K_{\alpha 1}$ (λ = 0.71073 Å) radiation was used to measure the scattering intensity. The crystal structure was refined with the SHELXTL package (35). Electrical resistivity, magneto-resistivity, Hall effect, and specific heat measurements were performed by using a Quantum Design Physical Property Measurement System DynaCool. The magnetization and magnetic susceptibility measurements were carried out with a Quantum Design Magnetic Property Measurement System (36). SEM and

EDX were taken with a FEI Scios DualBeam focused ion beam (FIB)/SEM operated at 15 kV.

ACKNOWLEDGMENTS. We thank Profs. James Allen and Zachary Fisk for helpful discussions. Materials synthesis and characterization at the University of California, San Diego (UCSD) were supported by US Department of Energy, Office of Basic Energy Sciences, Division of Materials Sciences and Engineering Grant DEFG02-04-ER46105. Transport, thermal, and magnetic measurements at UCSD were sponsored by the National Nuclear Security Administration under the Stewardship Science Academic Alliance Program through US Department of Energy Grant DE-NA0002909. Single crystalline X-ray diffraction measurements by W.X. at Louisiana State University (LSU) were supported by LSU startup funds. SEM, EDX, and FIB experiments by S.W. and Y.S.M. were supported by California Energy Commission EPIC Advance Breakthrough Award EPC-16-050 and were performed at San Diego Nanotechnology infrastructure, supported by National Science Foundation Grant ECCS-1542148.

1. Jaccarino V, Wertheim GK, Wernick JH, Walker LR, Arajs S (1967) Paramagnetic excited state of FeSi. *Phys Rev* 160:476–482.
2. Schlesinger Z, et al. (1993) Unconventional charge gap formation in FeSi. *Phys Rev Lett* 71:1748–1751.
3. Sales BC, et al. (1994) Magnetic, transport, and structural properties of $Fe_{1-x}Ir_xsi$. *Phys Rev B* 50:8207–8213.
4. Mandrus D, Sarrao JL, Migliori A, Thompson JD, Fisk Z (1995) Thermodynamics of FeSi. *Phys Rev B* 51:4763–4767.
5. Paschen S, et al. (1997) Low-temperature transport, thermodynamic, and optical properties of FeSi. *Phys Rev B* 56:12916–12930.
6. Takahashi Y, Moriya T (1979) A theory of nearly ferromagnetic semiconductors. *J Phys Soc Jpn* 46:1451–1459.
7. Fisk Z, et al. (1995) Kondo insulators. *Phys B Condens Matter* 206:798–803.
8. Varma CM (1994) Aspects of strongly correlated insulators. *Phys Rev B* 50:9952–9956.
9. Fu C, Doniach S (1995) Model for a strongly correlated insulator: FeSi. *Phys Rev B* 51:17439–17445.
10. Anisimov VI, Ezhov SY, Elfimov IS, Solovyev IV, Rice TM (1996) Singlet semiconductor to ferromagnetic metal transition in FeSi. *Phys Rev Lett* 76:1735–1738.
11. Wertheim GK, et al. (1965) Unusual electronic properties of FeSi. *Phys Lett* 18:89–90.
12. Kohgi M, Ishikawa Y (1981) Neutron scattering from FeSi. *Solid State Commun* 37:833–836.
13. Jarlborg T (1995) Low-temperature properties of ε-FeSi from ab initio band theory. *Phys Rev B* 51:11106.
14. Sun P, Wei B, Menzel D, Steglich F (2014) Resonant charge relaxation as a likely source of the enhanced thermopower in FeSi. *Phys Rev B* 90:245146.
15. Petrova AE, et al. (2010) Elastic, thermodynamic, and electronic properties of MnSi, FeSi, and CoSi. *Phys Rev B* 82:155124.
16. Mihalik M, et al. (1996) Magnetic properties and gap formation in FeSi. *J Magn Magn Mater* 157:637–638.
17. Bocellip S, Marabelli F, Spolenak R, Bauer E (1995) Evolution of the optical response from a very narrow gap semiconductor to a metallic material in $(Fe_xMn_{1-x})Si$. *MRS Online Proc Libr Archive* 402:361.
18. Schlesinger Z, et al. (1993) Unconventional charge gap formation in FeSi. *Phys Rev Lett* 71:1748–1751.
19. Hunt MB, et al. (1994) Low-temperature magnetic, thermal, and transport properties of FeSi. *Phys Rev B* 50:14933.
20. Brian CS, Olivier D, Michael AM, May AF (2011) Thermoelectric properties of Co-, Ir-, and Os-doped FeSi alloys: Evidence for strong electron-phonon coupling. *Phys Rev B* 83:125209.
21. Dietl T (2010) A ten-year perspective on dilute magnetic semiconductors and oxides. *Nat Mater* 9:965–974.
22. Sales BC, et al. (2012) Transport, thermal, and magnetic properties of the narrow-gap semiconductor $CrSb_2$. *Phys Rev B* 86:235136.
23. DiTusa JF, Friemelt K, Bucher E, Aeppli G, Ramirez AP (1998) Heavy fermion metal–kondo insulator transition in $FeSi_{1-x}Al_x$. *Phys Rev B* 58:10288–10301.
24. Fang Y, Wolowiec CT, Yazici D, Maple MB (2015) Chemical substitution and high pressure effects on superconductivity in the *Ln*OBiS_2 (*Ln*=La-Nd) system. *Novel Supercond Mater* 1:79–94.
25. Samuely P, Szabó P, Mihalik M, Hudáková N, Menovsky AA (1996) Gap formation in kondo insulator FeSi: Point contact spectroscopy. *Phys B Condens Matter* 218:185–188.
26. Wolfe R, Wernick JH, Haszko SE (1965) Thermoelectric properties of FeSi. *Phys Lett* 19:449–450.
27. Buschinger B, et al. (1997) Transport properties of FeSi. *Phys B Condens Matter* 230:784–786.
28. Ishizaka K, et al. (2005) Ultraviolet laser photoemission spectroscopy of FeSi: Observation of a gap opening in density of states. *Phys Rev B* 72:233202.
29. Arita M, et al. (2008) Angle-resolved photoemission study of the strongly correlated semiconductor FeSi. *Phys Rev B* 77:205117.
30. Klein M, et al. (2008) Evidence for itineracy in the anticipated kondo insulator FeSi: A quantitative determination of the band renormalization. *Phys Rev Lett* 101:046406.
31. Takahashi Y, Kanomata T, Note R, Nakagawa T (2000) Specific heat measurement of the single-crystalline FeSi and its theoretical analysis. *J Phys Soc Jpn* 69:4018–4025.
32. Marklund K, Larsson M, Byström S, Lindqvist T (1974) The specific heat of the binary compounds FeSi, CoSi, FeGe and CoGe. *Phys Scr* 9:47–50.
33. Koyama K, Goto T, Kanomata T, Note R (1999) Precise magnetization measurements of single-crystalline FeSi under high pressure. *J Phys Soc Jpn* 68:1693–1698.
34. Wilson KG (1975) The renormalization group: Critical phenomena and the kondo problem. *Rev Mod Phys* 47:773–840.
35. Sheldrick GM (2008) A short history of SHELX. *Acta Crystallogr Sect A Found Crystallogr* 64:112–122.
36. Fang Y, Yazici D, White BD, Maple MB (2015) Enhancement of superconductivity in $La_{1-x}Sm_xO_{0.5}F_{0.5}BiS_2$. *Phys Rev B* 91:064510.